Theoretical Model of the Effect of Combined Glenohumeral Bone Defects on Anterior Shoulder Instability: A Finite Element Approach

Piyush Walia,[1,2] Anthony Miniaci,[1,3] Morgan H. Jones,[1,3] Stephen D. Fening[2,4]

[1]Department of Biomedical Engineering, Lerner Cleveland Clinic, Cleveland, Ohio, [2]Austen BioInnovation Institute in Akron, 47 N Main Street, Akron, Ohio 44308, [3]Department of Orthopaedic Surgery, Cleveland Clinic, Cleveland, Ohio, [4]Department of Orthopaedic Surgery, Summa Health System, Akron, Ohio

Received 21 March 2012; accepted 15 October 2012
Published online 19 November 2012 in Wiley Online Library (wileyonlinelibrary.com). DOI 10.1002/jor.22267

ABSTRACT: The presence of either a Hill–Sachs or a bony Bankart defect has been indicated as a possible cause of subluxation and anterior shoulder dislocation. Previous studies investigated only the effects of isolated humeral or glenoid defects on glenohumeral instability. We investigated the effects on shoulder stability of both glenoid and humeral defects in the glenohumeral joint. A computer-based finite element approach was used to model the joint. A generic model was developed for cartilage and bone of the glenoid and humerus, using previously published data, and experiments were analyzed using static analysis with displacement control in the anterior-inferior direction. Simulations were run with a 50-N compressive load in the presence of both isolated and combined defects to analyze reaction forces and distance to dislocation. The distance to dislocation for normal joint was 13.6 mm at 90° abduction, which reduced to 9.7, 0, and 0 mm for largest isolated humerus defect, glenoid defect, and certain combined defects, respectively. For combined defects, stability ratio was decreased to 0% from 43%. Our results suggest that in the setting of combined bone defects, stability may be reduced more than what is known for isolated defects alone. J Orthop Res 31:601–607, 2013

Keywords: glenohumeral joint; shoulder; Hill–Sachs defect; instability; dislocation

The glenohumeral joint of shoulder is the most mobile joint in the body. Often this joint undergoes dislocation or subluxation associated with traumatic injury. Anterior shoulder dislocation accounts for ~98% of all shoulder dislocations.[1–3] A recent study showed that in the U.S. the incidence rate was 4.35/1,000 person-years. Nearly 1.7% of the population experiences an anterior shoulder dislocation.[4,5] The study also showed that the number of dislocations are almost double for military personnel and contact athletes.[5] Hill–Sachs and bony Bankart defects are two major types of compression fracture injuries reported during dislocation. The Hill–Sachs defect is a grooved defect from the posterior superior portion of the humeral head.[6] A Bankart defect is the detachment of the glenoid labrum from the glenoid rim and can also be associated with a fracture (bony Bankart defect) and loss of bone at the glenoid rim.[7] Nearly 62% of cases with recurrent dislocation have both Hill–Sachs and bony Bankart defects.[8,11]

Little consensus exists for the treatment of these two shoulder defects, due to limited available data. Some studies showed an inverse relationship between stability and size of the defect when an isolated defect is present. Itoi et al. analyzed the effect of the isolated bony Bankart defect on the stability of the glenohumeral joint, and Kaar et al. looked at the effect of a Hill–Sachs defect on the stability of the glenohumeral joint.[9,10] However, most patients have an unstable shoulder that has both Hill–Sachs and bony Bankart defects. Widaja et al.[11] were the first to document the correlation between Bankart and Hill–Sachs defects, but to date, no one has analyzed the effects of combined defects on stability. Treatment of unstable glenohumeral joint defects may require soft tissue repair, bone grafting, or both depending on the size and nature of the defects.[12–15] The most common treatment is isolated soft tissue repair, leaving the bone defects untreated. This partially results from the lack of evidence-based guidelines for the treatment of bone defects. Therefore, further data are needed to decide what sizes and combinations of bone defects cause significant instability that may require surgery.

It is impossible to mechanically test the combination of four different sizes of Hill–Sachs and bony Bankart defects each in a single cadaveric specimen. Therefore, a finite element (FE) approach was chosen. Our specific aim was to determine if a relationship exists between combined humeral head and glenoid bone defects and shoulder stability. We hypothesized that as the size of the both humeral head and glenoid bone defects increased, the glenohumeral joint's stability would decrease. We further hypothesized that the presence of both defects would magnify the reduction to joint stability to a greater extent than that of individual defect alone.

One or more authors has indicated a potential conflicts of interest: Anthony Miniaci and Morgan Jones have received unrestricted research grants from Arthrex, Donjoy, BREG, and Stryker. Anthony Miniaci has received royalties from Zimmer and Tenet, has received nonincome support from Arthrosurface, and is a consultant for Arthrosurface and Stryker. Stephen D. Fening is the co-founder and chief technology officer for Apto Orthopaedics. Grant sponsor: NFL Charities Medical Grant; Grant sponsor: Research Program Committee of the Cleveland Clinic (PI: Fening).
Correspondence to: Stephen D. Fening (T: 330-572-7544; F: 330-379-1192; E-mail: sfening@abiakron.org)

METHODS

Geometric Data for Model

A generic geometric model was created based on dimensions taken from data available in the literature for the male population (age range, 49–90 years; average age, 72 years).[16] The radius of curvature of articular bone and cartilages and thickness of cartilage for the glenoid and the humerus are shown in Table 1. The humerus cartilage is thicker at the center and thinner at the periphery of the humerus, whereas the opposite is true for the glenoid, being thinner at the center, in some cases so thin that it is referred to as a "bare spot."[16] The humeral head was modeled with an assumption of a sphere, as the available data are limited for an elliptical model. The glenoid was modeled using the width (AP dimension) of 29 mm and length (superior-inferior dimension) of 39 mm.[17,18] The glenohumeral and scapulothoracic joints move relative to one another at a 2:1 ratio during humero-thoracic abduction.[20] For example, if the arm abducts to a humero-thoracic angle of 90°, the glenohumeral joint will rotate 60°, and the scapular thoracic joint will rotate 30°. Likewise, a humero-thoracic abduction angle of 45° was calculated as the 30° glenohumeral joint rotation, and 15° rotation of the scapular thoracic joint. The arm was positioned prior to simulations.

FE Modeling

The glenoid cartilage was modeled using the software package Rhinoceros 3D (Robert McNeel & Associates, Seattle, WA), and the humerus cartilage was created using TrueGrid (XYZ Scientific Applications, Inc., Livermore, CA). Both models were meshed using TrueGrid having hybrid 3D hexahedral elements (C3D8H). These element types had eight nodes and six quadrilateral faces. The models were exported to the ABAQUS/6.9 (Simulia, Inc., Providence, RI) and assembled together. The model was assembled for two humero-thoracic abduction angles of the arm: 90° and 45°. The bones were considered as rigid bodies, and the material properties for the cartilage as a Neo-Hookean hyperelastic, incompressible material with an elastic modulus (E) of 10 MPa and Poisson's ratio (ν) of 0.4.[21–23] The material property constants C_{10} and D_{10} were calculated using Equations (1) and (2):

$$C_{10} = \frac{E}{4(1+\nu)} \tag{1}$$

$$D_{10} = \frac{E}{6(1-2\nu)} \tag{2}$$

The surface contact between the cartilage of the glenoid and humerus was assigned to be frictionless with mechanical hard contact and tangential behavior, and the Augmented Lagrange solver method was selected.[24] To minimize computational cost, frictionless contact was used; to test that it did not affect the variable of interest a sensitivity analysis was performed. The rigid bone and cartilage were coupled together to make a set of the glenoid bone and cartilage (glenoid set) and similarly a set was coupled for the humeral head bone and cartilage (humerus set). The simulation comprised three steps: contact, loading, and translation. In the contact step, contact was ensured between the two cartilage surfaces. In the loading step, a compressive force was applied on the humeral head (Z-axis, Figs. 1 and 2). In the translation step, the glenoid was stationary, and the humeral head was translated in the anterior-inferior direction (X-axis) while maintaining the compressive force constant. For validation of the model for glenoid defects, simulations were performed at 90° humero-thoracic abduction angle for internal and external rotation similar to Itoi et al. The arm positions for external rotation for defect sizes $¼^*R_g$, $½^*R_g$, $¾^*R_g$, and 1^*R_g were selected as 55°, 50°, 40°, and 25°, respectively. The internal rotation for individual defect was 0°, 5°, 5°, and 10°, respectively. The difference between the two studies is that Itoi et al. had the soft tissue intact in their model.

Creation of Defects

The defects were created using a plane to cut the area of the bone loss defect using TrueGrid software. The models were then imported and assembled in ABAQUS. The humerus was then rotated at an angle of 40.7° to account for the angle between the anatomical neck of the head and the humeral shaft.[19] Four individual defects were made to both the humerus and glenoid (Fig. 2). The defect sizes were selected similar to those from studies done by Kaar et al.[9] and Sekiya et al.[28] (humeral defects) and Itoi et al.[10] (glenoid defects). Osteotomy defects cuts were made through the surfaces of cartilage and bone (Fig. 2). Both sets of the defects were then combined, and simulations run with humero-thoracic abduction at 45° and 90°. The defects were created with respect to the radius of the glenoid (R_g) and humerus (R_h). Four different sizes of the defect for glenoid were created as $¼^*R_g$, $½^*R_g$, $¾^*R_g$, and 1^*R_g, and the defects for the humerus were $^1/_8{}^*R_h$, $^3/_8{}^*R_h$, $^5/_8{}^*R_h$, and $^7/_8{}^*R_h$. The combination of the defects and assembly view for 3D skeletal model are shown in Figure 1.

Loading and Boundary Conditions

A compressive force of 50 N was applied on the humeral head for the experimental procedure similar to the previous studies by Kaar et al.[9] and Itoi et al.[10] for the validation of the model. The simulation began with a contact step in which the humerus moved 1.2 mm in the medial–lateral direction to make contact with the glenoid surface. All other movements were constrained during this step. Then, in the loading step, the humerus set was free to translate in the lateral direction (Z-axis, Figs. 1 and 2), but all other movements and rotations were constrained. A 50 N compressive load was applied in the lateral direction. Finally, a translation step was performed by sliding the humerus in the

Table 1. Geometric Parameters for the Model[16]

Component	Radius of Curvature of Bone (mm)	Radius of Curvature of Cartilage (mm)	Thickness of Cartilage at Center (mm)
Glenoid	34.56	26.37	1.14
Humeral head	26.10	26.85	2.03

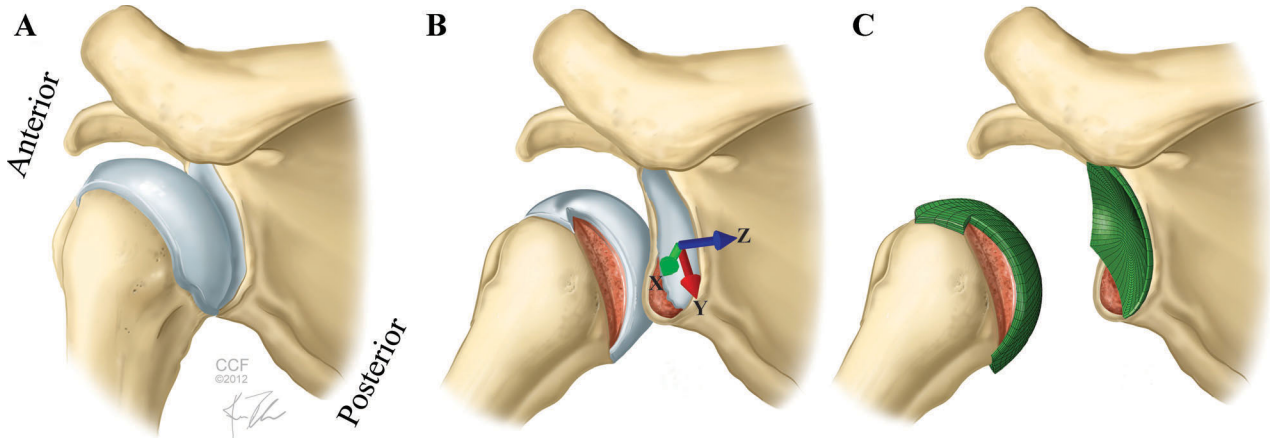

Figure 1. Normal joint at 0° abduction (A), joint with combination of Hill–Sachs and bony Bankart lesion at 90° abduction (B), and FE model mesh (green only) in presence of combined defects (C), where *X*-axis defines the translation in anterior-inferior direction (green arrow), and *Z*-axis points the direction of compression (blue arrow).

anterior-inferior direction (*X*-axis) to nearly 17 mm over the stationary glenoid.

Calculation of Stability Ratio

Stability ratio was defined as the ratio of the shear force to the compressive load acting on the glenoid, as in Equation (3).[10]

$$\text{Stability ratio} = \frac{\text{shear force}}{\text{compressive force}} \tag{3}$$

This shear force is the amount of force required to translate the humeral head in the anterior-inferior direction to dislocation, which is due to glenoid curvature, whereas, the compressive force is a force, normal to the glenoid, which compresses the joint. This mimics the effect of soft tissue stabilizers of the joint.

Point of Dislocation

The dislocation point was defined as the inflection point in the medial/lateral translation curve. The distance traveled by the humeral head during the translation step from the initial point until the point of dislocation was called the distance to dislocation. The horizontal axis (Fig. 3) signifies the

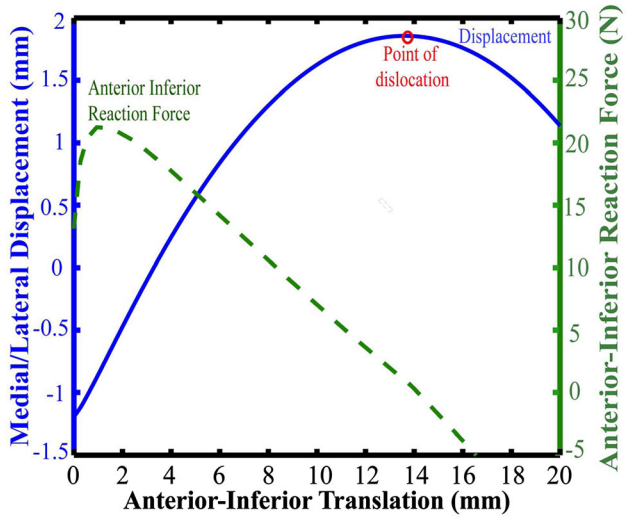

Figure 3. Medial/lateral displacement of humerus, dislocation point, and anterior-inferior reaction force acting on the humeral head during the translation of the humerus in the anterior-inferior direction.

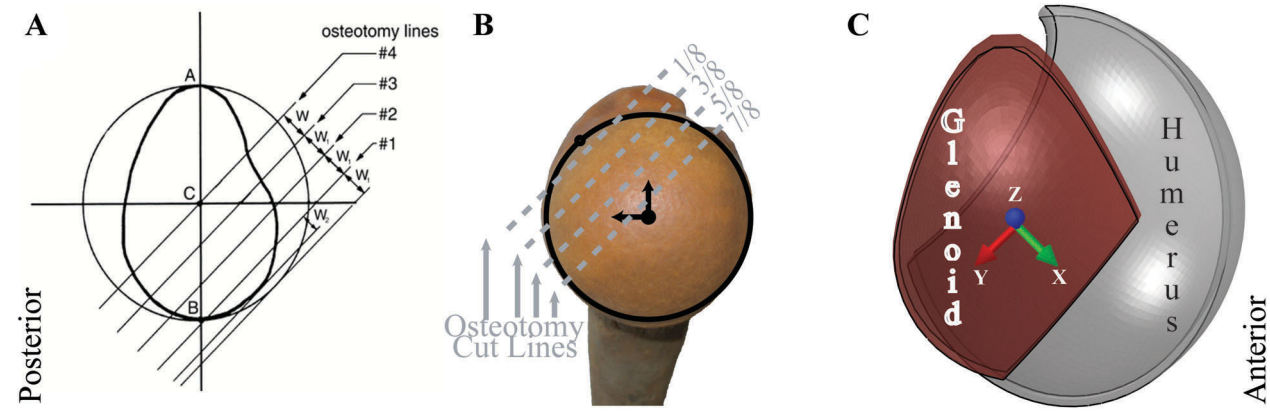

Figure 2. Bankart defect sizes adapted from Itoi et al.[10] (A), Hill–Sachs defect sizes adapted from Kaar et al. study[9] (B), and assembly view of combined defects (C), where *X*-axis (green arrow) shows the anterior-inferior translation direction, and *Z*-axis (blue arrow) signifies the medical compression.

anterior-inferior translational distance; the left vertical axis signifies the movement of the humerus in medial/lateral direction (mm), and the right axis is anterior-inferior reaction force (N). The inflection point was found using a spline interpolation curve fitting technique using Matlab/10.a (The MathWorks, Inc., Natick, MA).

RESULTS

Figure 4 shows a comparison of results for the percent intact translational distance to dislocation from our study and the study by Kaar et al.[9] for isolated Hill–Sachs defects. The results comparison for the reaction force between our study and that of the study by Itoi et al.[10] are shown in Figure 5. The results for the translational distance to dislocation in the presence of combined defects at 45° and 90° humero-thoracic abduction angles with neutral rotation are shown in Table 2a and b. The distances to dislocation for an intact joint at 45° and 90° humero-thoracic abduction of arm were 14.0 and 13.6 mm, respectively. This decreased to 0.0 mm at both 45° and 90° humero-thoracic abduction for the largest glenoid defects and various

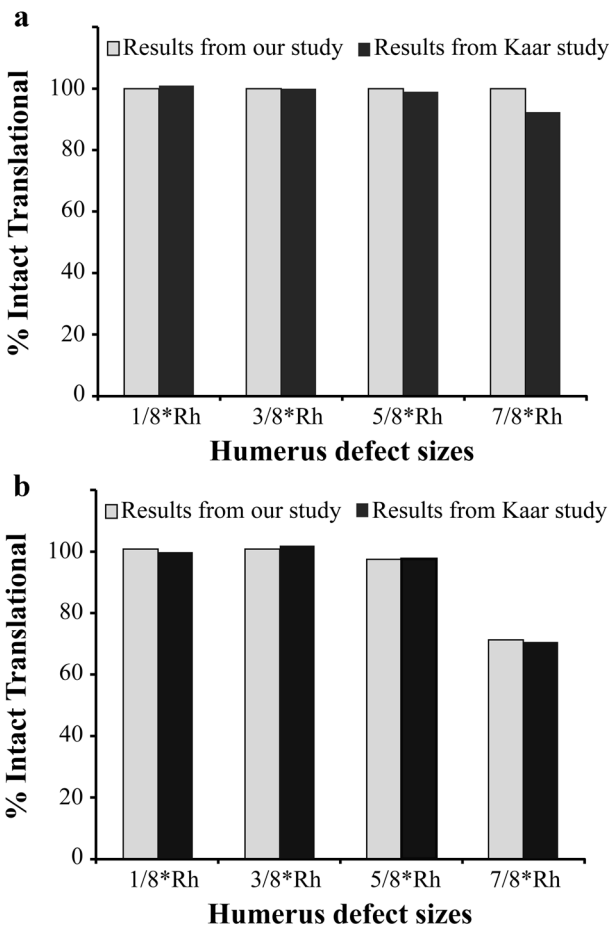

Figure 4. Percent intact translation for isolated Hill–Sachs defect at 45° (A) and 90° (B) humero-thoracic abduction and neutral rotation, which was calculated with respect to the intact joint translational distance, compared to results from the study by Kaar et al.[9]

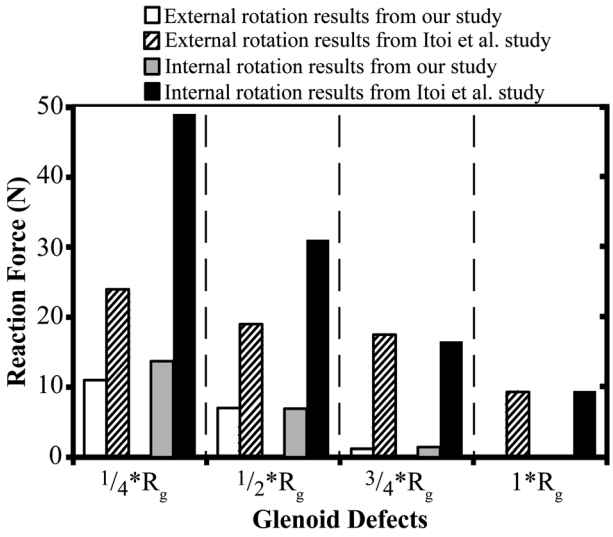

Figure 5. Net peak reaction force for the isolated bony Bankart defect at 90° humero-thoracic abduction compared with results from the study by Itoi et al.[10] for external and internal rotation.

combinations of defects. A distance to dislocation value of 0.0 mm signifies that the joint was completely unstable. The isolated bony Bankart defects had a major impact on the distance to dislocation as compared to that of isolated Hill–Sachs defects. At 90° humero-thoracic abduction, the distance to dislocation was reduced significantly in the presence of combined defects.

The stability ratio at 45° humero-thoracic abduction decreased from 44% to 0% for largest glenoid defect combinations only (Table 3a). The stability ratio for the intact joint was 43% at 90° humero-thoracic abduction and decreased to 0% for largest glenoid defect ($1^{*}R_{g}$) combinations and also the combination of $^{7}/_{8}{}^{*}R_{h}$ and $^{5}/_{8}{}^{*}R_{h}$ (Table 3b). The glenoid defects had more impact on the stability for the glenohumeral joint, whereas values of stability ratio were not affected by the humeral defect.

DISCUSSION

Many studies analyzed only the effects of either the isolated Hill–Sachs defect or the bony Bankart defect on shoulder stability.[9,10,27] It was reported in recent studies that the problem of recurrent dislocation is often caused by the presence of both defects.[8,11] The purpose of our study was to evaluate the theoretical stability of the glenohumeral joint with the presence of the two defects (bony Bankart and Hill–Sachs defects). Simulations were performed at two different arm positions of 45° and 90° humero-thoracic abduction. The simulations were stopped when the defect engaged. The point of engagement (Fig. 3) was the inflection point reflecting when the humerus "falls off" of the glenoid. The depth of the defect did not affect the results as the simulation was stopped prior to the point at which the humeral head would contact the bottom of

Table 2. Distance to Dislocation for Combined Defects (in Millimeters) at 45° (a) and 90° (b) Humero-Thoracic Abduction and Neutral Rotation

	Humeral Head Defects				
	Intact	$^{1}/_{8}{}^{*}R_{h}$	$^{3}/_{8}{}^{*}R_{h}$	$^{5}/_{8}{}^{*}R_{h}$	$^{7}/_{8}{}^{*}R_{h}$
(a) Glenoid Defects (45°)					
Intact	14.0	14.1	14.1	14.0	14.1
$^{1}/_{4}{}^{*}R_{g}$	10.5	10.6	10.7	10.6	10.6
$^{1}/_{2}{}^{*}R_{g}$	6.8	6.8	6.9	6.8	7.0
$^{3}/_{4}{}^{*}R_{g}$	2.4	2.5	2.4	2.5	2.6
$1{}^{*}R_{g}$	0.0	0.0	0.0	0.0	0.0
(b) Glenoid Defects (90°)					
Intact	13.6	13.7	13.6	13.3	9.7
$^{1}/_{4}{}^{*}R_{g}$	10.1	10.2	10.2	9.9	6.7
$^{1}/_{2}{}^{*}R_{g}$	6.3	6.4	6.3	6.1	3.0
$^{3}/_{4}{}^{*}R_{g}$	1.8	1.9	1.8	1.9	0.0
$1{}^{*}R_{g}$	0.0	0.0	0.0	0.0	0.0

the defect. This type of defect was chosen based on previously published biomechanical literature.[9,28] The distances to dislocation and peak reaction force in the anterior-inferior direction were recorded to measure the stability of the joint.

Comparison of our model to previously published mechanical testing data was an important component of the study. Our results for the isolated defects were compared with results from previous studies. The model boundary conditions mimicked each of the previous studies. Results showed conformity with those from the study by Kaar et al.[9]; values for the percent intact translation distance were similar and the same decreasing pattern for percent intact translation was seen as the size of the defect increased. However, the result for the largest isolated Hill–Sachs defect at 45° humero-thoracic abduction had a variation of 7%. The reason for this difference may be the generic model geometry of the joint. Modeling the humeral head as a sphere rather than ellipsoid may have an effect on glenohumeral biomechanics.

Results for the reaction force were compared with results from the study by Itoi et al.[10] Tests were performed at 90° humero-thoracic abduction of the arm with external, internal, and neutral rotation of arm. In prior studies, a similar trend was seen with the decreasing pattern of the reaction forces with increase in size of the defect. Another similarity was the lower values of the reaction force for internal rotation of arm versus the external rotation in both cases. However, the values for the reaction force from our study were lower, which could be due to the approximate geometry of our model and the absence of the soft tissues and glenohumeral capsule, unlike the study by Itoi et al.[10] The assumption of frictionless contact had nominimal impact on reaction force; the results were confirmed by doing a sensitivity test for cartilage friction of 0.001.[21]

Table 3. Stability Ratio for Combined Defects at 45° (a) and 90° (b) Humero-Thoracic Abduction and Neutral Rotation of Arm

	Humeral Head Defects				
	Intact	$^{1}/_{8}{}^{*}R_{h}$	$^{3}/_{8}{}^{*}R_{h}$	$^{5}/_{8}{}^{*}R_{h}$	$^{7}/_{8}{}^{*}R_{h}$
(a) Glenoid Defects (45°)					
Intact	0.44	0.44	0.44	0.44	0.44
$^{1}/_{4}{}^{*}R_{g}$	0.32	0.31	0.32	0.32	0.32
$^{1}/_{2}{}^{*}R_{g}$	0.17	0.18	0.17	0.18	0.17
$^{3}/_{4}{}^{*}R_{g}$	0.03	0.04	0.03	0.04	0.03
$1{}^{*}R_{g}$	0.00	0.00	0.00	0.00	0.00
(b) Glenoid Defects (90°)					
Intact	0.43	0.42	0.43	0.43	0.43
$^{1}/_{4}{}^{*}R_{g}$	0.30	0.30	0.30	0.31	0.30
$^{1}/_{2}{}^{*}R_{g}$	0.16	0.16	0.16	0.17	0.19
$^{3}/_{4}{}^{*}R_{g}$	0.02	0.02	0.02	0.03	0.00
$1{}^{*}R_{g}$	0.00	0.00	0.00	0.00	0.00

The distance to dislocation was affected by the presence of both Hill–Sachs and bony Bankart defects. At 45° humero-thoracic abduction, the distance to dislocation decreased from 14.0 to 0.0 mm for bony Bankart defect but stayed unaffected by isolated Hill–Sachs defect. However, at 90° humero-thoracic abduction, it decreased from 14.0 to 9.9 mm for the isolated Hill–Sachs defect showing that increased abduction had an impact on stability. The distance to dislocation decreased with increasing size of the bony Bankart defect. It reduced from 14.0 to 0.0 mm for the largest bony Bankart defect. This showed that glenoid defects have a greater impact on the stability of the joint than a Hill–Sachs defect. The distance to dislocation for some of the combinations of the defects at 90° humero-thoracic abduction decreased from 14.0 to 0.0 mm.

The stability ratio for a normal intact glenohumeral joint was found to be 43% and 44% for 90° and 45° humero-thoracic abduction angles, respectively. In the presence of isolated defects in the glenoid, the stability decreased to 0% for the largest defect (R_g) at both abduction angles. The isolated Hill–Sachs defects did not have substantial effect on values of the stability ratio in the positions that we tested. However, these defects could have a greater effect on stability in greater degrees of external rotation, as patients clinically exhibit increasing apprehension as the arm is externally rotated.[25,26] The results indicated that combined defects were more unstable than isolated glenoid defects. While glenoid defects affected stability to the same degree independent of arm position, humeral head defects had less of an effect on stability at 45° compared to 90° humero-thoracic abduction angle.

Our study provides information about the stability of the joint and the translational distance to dislocation for the combined defects. Itoi et al.[10] stated that defects with 21% bone loss or higher will need better repair treatments so as to maintain an effective length of the anterior arc of the bone. This surgery can be done through bone grafting or by elongation of the capsoligamentous structures. But defects below 21% of bone loss can be fixed by soft tissue repairs. Similar to the results found by the Itoi study, Kaar et al.[9] stated that a defect size greater than $^5/_8{}^*R_h$ of the humeral head may need a surgical treatment to fix the defect; otherwise, the patient may face the problems of recurrent shoulder instability. Also, the results were similar to those of Sekiya et al.[28] showing that defect size $^3/_8{}^*R_h$ had no effect on stability ratio. The results of our study showed that the stability is lowered even for the combination of two smaller defects. At 90° humero-thoracic abduction angle, the combination of $¼{}^*R_g$ with $^5/_8{}^*R_h$ and $^7/_8{}^*R_h$ had distance to dislocation reduced to 9.9 and 6.7 mm, respectively, from 14 mm. Hence, the treatment options suggested by them may not be valid for some cases when both defects are present together.

These findings give theoretical insight to the biomechanical behavior of shoulder stability in the presence of both humeral head and glenoid bone defects. One limitation of our study is that it did not include rotational movements of the arm (external and internal rotations). Such a study has the potential to help surgeons to better understand the instability of this joint under different conditions of defects if we look at the external and internal rotation of the arm. Better knowledge of these defects will be helpful in the choice of successful treatment options and reducing relapse for the patient. Future studies incorporating different rotations to assess shoulder stability will be performed to expand this model. Specimen specific approaches will be incorporated in future studies to understand the changes in biomechanics and stress of the joint.

REFERENCES

1. Walton J, Paxinos A, Tzannes A, et al. 2002. The unstable shoulder in the adolescent athlete. Am J Sports Med 30:758–767.
2. VandenBerghe G, Hoenecke HR, Fronek J. 2005. Glenohumeral joint instability: the orthopedic approach. Semin Musculoskelet Radiol 9:34–43.
3. Cofield RH, Kavanagh BF, Frassica FJ. 1985. Anterior shoulder instability. Instr Course Lect 34:210–227.
4. Wilson SR. 14 Dec. 2009. Dislocation, shoulder: Emedicine emergency medicine. EMedicine—Medical Reference Web. 01 Nov. 2010.
5. Owens BD, Dawson L, Burks R, et al. 2009. Incidence of shoulder dislocation in the United States military: demographic considerations from a high-risk population. J Bone Joint Surg Ser A 91:791–796.
6. Hill HA, Sachs MD. 1940. The grooved defect of the humeral head. Radiology 35:690–700.
7. Rowe CR, Patel D, Southmayd WW. 1978. The Bankart procedure: a long-term end-result study. J Bone Joint Surg Am 60:1–16.
8. Rowe CR, Zarins B, Ciullo JV. 1984. Recurrent anterior dislocation of the shoulder after surgical repair. Apparent causes of failure and treatment. J Bone Joint Surg Am 66:159–168.
9. Kaar SG, Fening SD, Jones MH, et al. Effect of humeral head defect size on glenohumeral stability: a cadaveric study of simulated Hill–Sachs defects. Am J Sports Med 38:594–599.
10. Itoi E, Lee SB, Berglund LJ, et al. 2000. The effect of a glenoid defect on anteroinferior stability of the shoulder after Bankart repair: a cadaveric study. J Bone Joint Surg Am 82:35–46.
11. Widjaja AB, Tran A, Bailey M, et al. 2006. Correlation between Bankart and Hill–Sachs lesions in anterior shoulder dislocation. ANZ J Surg 76:436–438.
12. Pritchett JW, Clark JM. 1987. Prosthetic replacement for chronic unreduced dislocations of the shoulder. Clin Orthop Relat Res 216:89–93.
13. Kropf EJ, Sekiya JK. 2007. Osteoarticular allograft transplantation for large humeral head defects in glenohumeral instability. Arthroscopy 23:322.e1–322.e5.
14. Bigliani LU, Newton PM, Steinmann SP, et al. 1998. Glenoid rim lesions associated with recurrent anterior dislocation of the shoulder. Am J Sports Med 26:41–45.
15. Izquierdo R, Voloshin I, Edwards S, et al. 2010. Treatment of glenohumeral osteoarthritis. J Am Acad Orthop Surg 18:375–382.

16. Soslowsky LJ, Flatow EL, Bigliani LU, et al. 1992. Articular geometry of the glenohumeral joint. Clin Orthop Relat Res 285:181–190.
17. De Wilde LF, Berghs BM, Audenaert E, et al. 2004. About the variability of the shape of the glenoid cavity. Surg Radiol Anat 26:54–59.
18. Iannotti JP, Gabriel JP, Schneck SL, et al. 1992. The normal glenohumeral relationships. An anatomical study of one hundred and forty shoulders. J Bone Joint Surg Am 74:491–500.
19. Pearl ML, Volk AG. 1996. Coronal plane geometry of the proximal humerus relevant to prosthetic arthroplasty. J Shoulder Elbow Surg 5:320–326.
20. Di Giacomo G, Pouliart N, Costantini A, et al., editors. 2008. Atlas of functional shoulder anatomy [electronic resource]. Milan; New York: Springer; XVI, p 90.
21. Buchler P, Ramaniraka NA, Rakotomanana LR, et al. 2002. A finite element model of the shoulder: application to the comparison of normal and osteoarthritic joints. Clin Biomech (Bristol, Avon) 17:630–639.
22. Kempson GE. 1982. Relationship between the tensile properties of articular cartilage from the human knee and age. Ann Rheum Dis 41:508–511.
23. Anderson AE, Ellis BJ, Maas SA, et al. 2010. Effects of idealized joint geometry on finite element predictions of cartilage contact stresses in the hip. J Biomech 43:1351–1357.
24. Anderson AE, Ellis BJ, Maas SA, et al. 2008. Validation of finite element predictions of cartilage contact pressure in the human hip joint. J Biomech Eng 130:1–25.
25. Farber AJ, Castillo R, Clough M, et al. 2006. Clinical assessment of three common tests for traumatic anterior shoulder instability. J Bone Joint Surg Am 88:1467–1474.
26. Tzannes A, Murrell GA, Farber AJ, et al. 2002. Clinical examination of the unstable shoulder clinical assessment of three common tests for traumatic anterior shoulder instability. Sports Med 32:447–457.
27. Sekiya JK, Jolly J, Debski RE. 2012. The effect of a Hill–Sachs defect on glenohumeral translations, in situ capsular forces, and bony contact forces. Am J Sports Med 40:388–394.
28. Sekiya JK, Wickwire AC, Stehle JH, et al. 2009. Hill–Sachs defects and repair using osteoarticular allograft transplantation: biomechanical analysis using a joint compression model. Am J Sports Med 37:2459–2466.